

RAPID COMMUNICATION

Differential Patterns of Subcortical Activity Evoked by Glial GLT-1 Blockade in Prelimbic and Infralimbic Cortex: Relationship to Antidepressant-Like Effects in Rats

Júlia Gasull-Camós, Maria Luisa Soto-Montenegro, Marta Casquero-Veiga, Manuel Desco, Francesc Artigas, Anna Castañé

Department of Neurochemistry and Neuropharmacology, CSIC-Institut d'Investigacions Biomèdiques de Barcelona, Barcelona, Spain (Drs Artigas and Castañé and Ms Gasull-Camós); Institut d'Investigacions Biomèdiques August Pi i Sunyer, Barcelona, Spain (Drs Artigas and Castañé and Ms Gasull-Camós); Centro de Investigación Biomédica en Red de Salud Mental, Instituto de Salud Carlos III, Madrid, Spain (Drs Artigas, Castañé, Desco and Soto-Montenegro, Ms Casquero-Veiga and Ms Gasull-Camós); Instituto de Investigación Sanitaria Gregorio Marañón, Madrid, Spain (Drs Desco and Soto-Montenegro and Ms Casquero-Veiga); Departamento de Bioingeniería e Ingeniería Aeroespacial, Universidad Carlos III de Madrid, Spain (Dr Desco); Centro Nacional de Investigaciones Cardiovasculares, Madrid, Spain (Dr Desco).

Correspondence: Anna Castañé, PhD, Department of Neurochemistry and Neuropharmacology, Rosselló 161 6th Floor, 08036 Barcelona, Spain (acfnqi@iibb.csic.es).

Abstract

Background: Glutamatergic neurotransmission has emerged as a novel target in antidepressant drug development, with a critical role of the ventral anterior cingulate cortex. We recently reported that blockade of the astrocytic glutamate transporter GLT-1 with dihydrokainic acid in infralimbic cortex (rodent equivalent of ventral anterior cingulate cortex), but not in the adjacent prelimbic cortex, evoked robust antidepressant-like effects through α -amino-3-hydroxy-5-methyl-4-isoxazolepropionic acid receptor activation and increased serotonin release.

Methods: 2-deoxy-2- ^{18}F -fluoro-D-glucose-positron emission tomography and computed tomography in 36 male Wistar rats microinfused bilaterally in prelimbic cortex or infralimbic cortex with dihydrokainic acid or vehicle.

Results: Dihydrokainic acid microinfusion in infralimbic cortex and prelimbic cortex evoked dramatically different regional patterns of subcortical activity. In infralimbic cortex, dihydrokainic acid selectively affected midbrain areas, whereas in prelimbic cortex it affected the basal ganglia, the thalamus, and both superior and inferior colliculi.

Conclusions: These results highlight the differential connectivity of infralimbic and prelimbic cortex with subcortical brain regions and support the involvement of infralimbic cortex-midbrain pathway in the antidepressant-like effects of dihydrokainic acid.

Keywords: infralimbic, prelimbic, glutamate transporter-1, FDG-PET, dihydrokainic acid

Received: May 26, 2017; Revised: July 18, 2017; Accepted: July 28, 2017

© The Author(s) 2017. Published by Oxford University Press on behalf of CINP.

This is an Open Access article distributed under the terms of the Creative Commons Attribution Non-Commercial License (<http://creativecommons.org/licenses/by-nc/4.0/>), which permits non-commercial re-use, distribution, and reproduction in any medium, provided the original work is properly cited. For commercial re-use, please contact journals.permissions@oup.com

Significance Statement

The glutamatergic system is a potential target to develop fast-acting antidepressants. On the other hand, glial cells tightly control glutamatergic synapses. We recently reported that boosting glutamatergic neurotransmission by inhibiting astrocytic glutamate uptake in a ventral area of the rat prefrontal cortex (infralimbic, IL; but not in the neighboring prelimbic cortex, PrL) evoked rapid and robust antidepressant-like effects. Using microPET scan, we show that the blockade of astrocytic glutamate uptake in IL and PrL evokes dramatically different patterns of brain activity, showing at the same time that IL-midbrain circuits (possibly involving serotonergic neurotransmission) underlie the reported antidepressant effects.

Introduction

The glutamatergic system is emerging as a promising venue for the development of fast-acting antidepressant treatments, given the immediate and persistent antidepressant effects of the noncompetitive N-methyl-D-aspartate receptor antagonist ketamine (Zarate et al., 2006). Its unique properties appear to result from the activation of α -amino-3-hydroxy-5-methyl-4-isoxazolepropionic acid (AMPA) receptors by a metabolite (2S,6S;2R,6R)-hydroxynorketamine (Zanos et al., 2016) and by an increased synaptic plasticity evoked by mTOR signaling in rat medial prefrontal cortex (mPFC) (Li et al., 2010).

Ventral regions of the anterior cingulate cortex (vACC) seem to play a crucial role in the pathophysiology and treatment of major depressive disorder. Neuroimaging studies have reported controversial findings on the energy metabolism of that area in major depressive disorder patients. A reduced activity of the subgenual vACC was first described (Drevets et al., 1997; Ongür et al., 1998), whereas further studies reported an increased activity of the adjacent Brodmann area 25, which was normalized after effective treatment (Seminowicz et al., 2004; Mayberg et al., 2005). Likewise, optogenetic stimulation of the infralimbic cortex (IL, rodent equivalent of vACC) in rats mimicked the antidepressant-like effects of systemic ketamine administration (Fuchikami et al., 2015).

In line with these observations, we recently reported that the local single-point blockade of the astrocytic glutamate transporter GLT-1 with dihydrokainic acid (DHK) in rat IL evoked immediate and robust antidepressant-like effects in the forced swim and novelty suppressed feeding tests, associated with a marked elevation of serotonin (5-HT) release (Gasull-Camós et al., 2017). Behavioral and neurochemical effects were blocked and mimicked, respectively, by local microinfusion of the AMPA/KA antagonist NBQX and S-AMPA. Interestingly, neither effect occurred when DHK or S-AMPA were locally applied in the adjacent prelimbic cortex (PrL) using exactly the same methodology and drug doses as in IL experiments (Gasull-Camós et al., 2017).

Using 2-deoxy-2- 18 F-fluoro-D-glucose (18 FDG) positron emission tomography (PET) in rats, we examined the changes in brain activity induced by DHK microinfusion in IL and PrL using the same application procedure than in our previous report. Given that antidepressant-like effects of DHK were associated to increased 5-HT release and were prevented by prior 5-HT synthesis inhibition with pCPA (Gasull-Camós et al., 2017), the working hypothesis was that DHK application in IL (but not in PrL) would increase the activity of midbrain 5-HT neurons, remarkably sensitive to changes of neuronal activity in the mPFC (Hajós et al., 1998; Celada et al., 2001; Warden et al., 2012).

Methods

Animals

Male Wistar rats (Charles River) weighing 280 to 330 g at the time of surgery were used. Rats were housed in a temperature- and

humidity-controlled vivarium with a 12-h-light/-dark cycle and with food and water ad libitum (unless otherwise stated). Experiments were performed according to the guidelines of the European Union Council Directive 2010/63/EU for care of laboratory animals and after approval by the Ethics Committee for Animal Experimentation of Hospital Gregorio Marañón, Madrid, Spain.

Surgery

Anesthetized rats (sodium pentobarbital, 60 mg/kg i.p.) were placed into a stereotaxic frame. Stainless-steel 22-gauge bilateral guide cannulae (Plastics One) were implanted in the cingulate cortex: AP +3.2; ML \pm 0.75; DV -2.4 (Paxinos and Watson, 2005) as reported (Gasull-Camós et al., 2017). The coordinates were taken from bregma and the skull. Guide cannulae were fixed with 3 stainless-steel screws using dental acrylic. A dummy cannula was inserted inside the guide cannula and removed and reinserted daily to prevent occlusion. After surgery, rats were allowed 7 days of recovery.

Microinfusions

DHK was purchased from Tocris and dissolved in PBS 10x (Gasull-Camós et al., 2017). The microinfusion cannulae (28 gauge) extended 1.5 or 3 mm beyond the guide cannulae for PrL or IL local administration (DV: -3.9 or -5.4, respectively). The day previous to drug microinfusion and 18 FDG-PET testing, a mock infusion was performed. On the testing day, an infusion/withdrawal pump (Harvard Apparatus) was used to bilaterally administer DHK or PBS into the PrL or IL cortex through two 100- μ L Hamilton syringes connected to the microinfusion cannula via 0.28-mm ID polyethylene tubing. A volume of 0.5 μ L/hemisphere was administered over 1 minute, and microinfusion cannulae were left in place for 3 minutes to allow drug diffusion.

In Vivo Imaging Studies

PET studies were acquired with a small animal PET/computed tomography (CT) scanner (ARGUS PET/CT, SEDECAL). 18 FDG (~37 MBq; IBA Molecular Spain S.A.) was injected through the tail vein 10 minutes after completing the DHK or PBS infusion. After 45 minutes of uptake, animals were scanned under anesthesia with sevoflurane (3% induction, 1.5% maintenance in 100% O₂) for 45 minutes. Images were reconstructed by using a 2D-OSEM algorithm, full width half maximum of 1.45 mm, with a voxel size of 0.3875 \times 0.3875 \times 0.775 mm and an energy window of 400 to 700 keV. Decay and dead-time corrections were applied.

CT studies were acquired immediately before each PET scan with the same scanner to facilitate PET image registration. Acquisition parameters were 340 mA, 40 kV, 360 projections, 8 shots, and 200 μ m of resolution. CT images were reconstructed

using an FDK algorithm (isotropic voxel size of 0.121 mm) (Hadar et al., 2017).

PET Preprocessing and Analysis

PET scans were preprocessed as previously described (Hadar et al., 2017). Briefly, PET images were spatially co-registered to a random reference CT scan. A whole brain mask segmented on a magnetic resonance scan registered to the same reference CT scan was applied to all PET images to eliminate voxels outside the brain. Afterwards, PET images were smoothed with an isotropic Gaussian filter (2 mm full width half maximum).

Voxel value normalization consisted of standardizing PET intensity data to a brain region without statistically significant differences between groups (nonsignificant area [NSA]) obtained by an iterative method (Borghammer et al., 2009). First, PET data were normalized to global mean brain intensity and analyzed with a voxel-by-voxel analysis using SPM12 (<http://www.fil.ion.ucl.ac.uk/spm/software/spm12/>). Groups were compared using a 2-sample t test ($P < .05$, uncorrected). Then, a mask of the NSA was acquired from the resulting T-maps, excluding statistically significant clusters. Next, the NSA mask was used to normalize the original smoothed PETs, and the obtained images were reanalyzed with the same SPM protocol. Subsequently, an NSA mask from these second T maps was obtained, and we repeated the whole process until the fourth iteration, which was accepted as the final result of the analysis. Statistics were not corrected for multiple comparisons because of the lack of validation with rodent brain data of multiple comparison correction methods, such as familywise error rate or false discovery rate (Romero et al., 2011), and also because of the ethical demand to minimize the number of animals (Hadar et al., 2017). Thus, although this leads to a reduction in power, it prevents an underestimation of the statistical significance. Significant regions larger than 50 activated connected voxels were considered.

A region of interest analysis was performed to determine the intragroup global metabolic differences. Whole brain and NSA masks were used for this analysis. Whole brain data were normalized to the average NSA intensity. Global differences were assessed by means of a t test with a threshold for statistical significance set at $P < .05$.

Results

In Vivo Study of the DHK Effects

Measurements based on global alterations for whole brain metabolism showed no significant differences between treatment and vehicle groups, as shown by 2-sample t test. Thus, the microinfusion of DHK in PrL did not change the overall uptake of ^{18}F FDG compared with controls (DHK: 1.0078 ± 0.0009 ; PBS: 1.0081 ± 0.0007 ; $P = .825$) and neither did the microinfusion of DHK in IL (DHK: 1.0078 ± 0.0003 ; PBS: 1.0082 ± 0.0004 ; $P = .405$).

Despite there were no differences in the average global uptake of ^{18}F FDG, significant differences of the local metabolism were observed after DHK microinfusion. Thus, the microinfusion of DHK in PrL increased glucose metabolism in the prefrontal cortex ($T = 6.42$) and the cerebellum ($T = 3.13$). Conversely, PrL DHK application reduced glucose metabolism in the nucleus accumbens, the dorsal striatum (caudate-putamen), the thalamus, the ventral hippocampus, and the superior and inferior colliculi ($T = 5.1$) as well as in anterior cerebellar regions ($T = 2.46$) (Figure 1; Table 1). On the other hand, the microinfusion of DHK in IL produced an increase of glucose metabolism in the IL itself and the olfactory nucleus ($T = 2.61$) as well as in the temporal cortex ($T = 5.16$). A reduction of ^{18}F FDG uptake occurred in the periaqueductal gray matter (PAG), the midbrain region ($T = 3.77$), the somatosensory cortex ($T = 2.47$), and the cerebellum ($T = 2.42$) (Figure 1; Table 1).

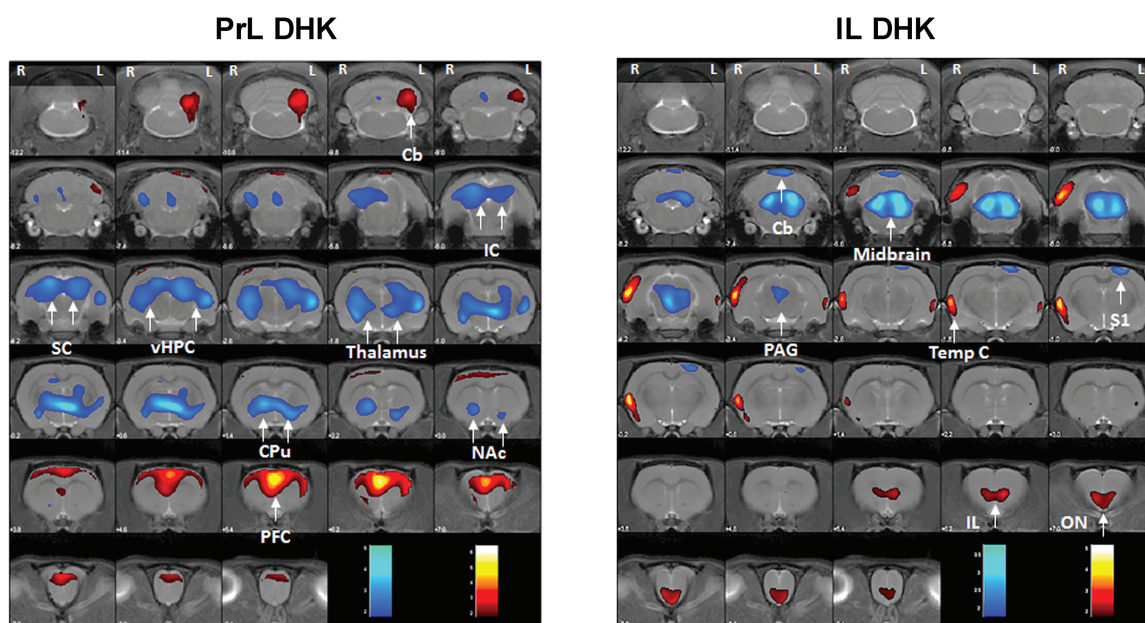


Figure 1. Changes in brain metabolic activity. Voxel-based SPM results in T-maps overlaid on a T2 magnetic resonance image, showing the changes in glucose metabolism due to dihydrokainic acid (DHK) administration in prelimbic (PrL, left) or infralimbic (IL, right). The color bars in the right represent the T values corresponding to lower (blue) and higher (red) 2-deoxy-2- ^{18}F -fluoro-D-glucose (^{18}F FDG) uptake ($P < .05$ [unc.]; $k = 50$ voxels). Brain regions: Cerebellum (Cb), caudate-putamen (CPu), inferior colliculus (IC), infralimbic cortex (IL), nucleus accumbens (NAc), olfactory nucleus (ON), periaqueductal gray matter (PAG), prefrontal cortex (PFC), superior colliculus (SC), somatosensory cortex (S1), temporal cortex (Temp C), thalamus, ventral hippocampus (VHPC).

Table 1. Glucose Metabolism Changes after DHK Administration in PrL or IL Cortices

	ROI	k	Side	↑/↓	T	P	FWE
PrL	PFC	1210	R & L	↑	6.42	<.001	0.009
	Cb	308	L	↑	3.13	.003	0.796
	NAc	2331	R & L	↓	5.1	<.001	0.07
	CPu						
	thalamus						
	vHPC						
IL	SC and IC						
	Cb		R & L	↓	2.46	.012	0.976
	ON	313	R & L	↑	5.16	<.001	0.092
	IL						
	Temp C	375	R	↑	2.61	.01	0.967
	PAG	870	R & L	↓	3.77	.001	0.524
	midbrain						
	S1	83	L	↓	2.47	.013	0.981
Cb	62	R & L	↓	2.42	.014	0.984	

Abbreviations for brain regions: Cb, cerebellum; CPu, caudate-putamen; IC, inferior colliculus; IL, infralimbic cortex; NAc, nucleus accumbens; ON, olfactory nucleus; PAG, periaqueductal gray matter; PFC, prefrontal cortex; SC, superior colliculus; S1, primary somatosensory cortex; Temp C, temporal cortex; vHPC, ventral hippocampus. Other abbreviations: FWE, p value after family wise error correction; k, cluster size; ROI, region of interest.

Discussion

The present study shows that blockade of the astroglial glutamate transporter GLT-1 with DHK in IL and PrL affects brain activity in a remarkably different manner, as assessed by micro-PET scan with ¹⁸FDG. In particular, the areas affected by DHK application in IL may reflect the brain circuitry responsible for the antidepressant-like effects and increased 5-HT release evoked by this procedure (Gasull-Camós et al., 2017).

The present and preceding observations add to previous studies supporting a crucial role of astrocytes in synaptic transmission and animal behavior (Oliveira et al., 2015), an effect due to their ability to control glutamatergic synapses (Perea and Araque, 2010). Hence, the astrocytic glutamate transporters GLT-1 and GLAST are responsible for the uptake of most synaptic glutamate, with a minor role of the neuronal transporter EAAC1 (Danbolt, 2001).

GLT-1 blockade markedly elevated energy metabolism in the application areas, an effect likely related to the increased glutamate outflow produced by DHK (Gasull-Camós et al., 2017) and the subsequent activation of local excitatory receptors, leading to an increased neuronal discharge and energy consumption. Despite that we used the same experimental procedure and that DHK elevates extracellular glutamate to the same extent in both subdivisions (Gasull-Camós et al., 2017), DHK application in PrL markedly activated neighboring PFC areas, such as cingulate and motor cortices, whereas DHK application in IL evoked a more restricted activation pattern. This difference may possibly be related to the inhibitory role of IL on PrL activity (Ji and Neugebauer, 2012), thus preventing an excitatory wave expanding outside the application site, as after PrL application.

In addition to their respective application sites, GLT-1 blockade affected several cortical and subcortical regions in a differential manner, sometimes with opposite activity changes (increase and decrease in cortical/cerebellar and subcortical areas, respectively, as shown in Figure 1 and Table 1). DHK application in PrL mainly affected structures from basal ganglia circuits (e.g., dorsal and ventral striatum, thalamus) as well as the ventral hippocampus, the colliculi, and cerebellum. In contrast, GLT-1 blockade in IL mainly reduced metabolic activity in midbrain structures, such as the PAG, yet increased it in temporal

cortex and olfactory nucleus. It is of note that some effects seem to be lateralized, like the reduced left S1 and the increased right temporal cortex glucose metabolism, after IL DHK. Interestingly, clinical studies in repeated transcranial magnetic stimulation showed that the left and right frontal cortices require different frequency ranges of stimulation (high/excitatory and low/inhibitory, respectively) to achieve antidepressant efficacy (Chen et al., 2013). Moreover, greater activity of left PFC was predictive of favorable response to antidepressants (Hohn-Saric et al., 2001). Although these studies focused on PFC, it would be interesting to study the contribution of brain activity asymmetry in other cortical regions for the antidepressant response.

The comparable elevation of extracellular glutamate concentration in IL and PrL after GLT-1 blockade (Gasull-Camós et al., 2017) indicates that differential effects of DHK in IL vs PrL in terms of animal behavior, elevation of 5-HT release, and brain areas affected are not due to a distinct control of synaptic glutamate by GLT-1 in each of these cortical areas. Most convincingly, these differences are due to the different role of IL and PrL in PFC functions (Dalley et al., 2004), resulting from their differential connectivity with subcortical structures involved in cognitive and emotional processing (Vertes, 2004; Gabbott et al., 2005). Additionally, a distinct reactivity of pyramidal neurons or local microcircuits in IL and PrL to the glutamate increase evoked by GLT-1 blockade might be involved, given the presence of reciprocal connections between both PFC subdivisions (Gabbott et al., 2003) and the inhibitory role of IL on PrL activity (Ji and Neugebauer, 2012).

The reduction of activity in subcortical structures after GLT-1 blockade in IL and PrL appears inconsistent with the excitatory nature of descending pyramidal inputs. However, some of these structures (e.g., dorsal striatum, nucleus accumbens, PAG) are composed essentially of GABAergic neurons, while others (e.g., thalamus) are tonically inhibited by GABAergic inputs from substantia nigra reticulata, ventral pallidum, and the thalamic reticular nucleus. Therefore, descending cortical excitatory inputs may activate inhibitory neurotransmission in input and output structures of the basal ganglia, thus leading to a reduced neuronal activity and energy consumption.

Likewise, the reduced energy metabolism in midbrain produced by DHK application in IL seems at variance with the elevated 5-HT release produced by this procedure (Gasull-Camós et al.,

2017). This 5-HT elevation, together with the cancellation of antidepressant-like effects of IL DHK application by prior 5-HT synthesis inhibition, led us to hypothesize an increased activity of raphe 5-HT neurons. Contrary to these expectations, the present data indicate a marked and overall reduction of energy metabolism in PAG (whose ventral part includes the dorsal raphe nucleus) after IL DHK application. One possible confounding factor is the use of anesthesia in the present study, the only experimental difference with respect to the previous study. However, this apparent contradiction may be partly explained by the complex neuronal connectivity between the mPFC and raphe 5-HT neurons, also including reciprocal PrL-IL connectivity, as stated above. Indeed, electrical stimulation at physiological rates (e.g., ~1 Hz) of the mPFC, particularly in its IL subdivision, led to a majority of inhibitory responses in dorsal raphe 5-HT neurons recorded *in vivo* in anesthetized rats. Inhibitory responses were mediated by local GABA_A inputs (Hajós et al., 1998; Varga et al., 2001) as well as by self-inhibitory responses mediated by 5-HT_{1A} autoreceptors (Celada et al., 2001). Actually, raphe 5-HT neurons receive local GABA contacts (Harandi et al., 1987), which inhibit 5-HT neurons (Liu et al., 2000). Contacts among cells of each neuronal subtype (GABA-GABA and 5-HT-5-HT) have also been reported (Harandi et al., 1987). Therefore, an IL-driven inhibition of PAG activity may attenuate GABA inputs onto 5-HT neurons, leading to an overall disinhibition of the 5-HT system and increased forebrain 5-HT release, as previously observed (Gasull-Camós et al., 2017). The activation of 5-HT neurons may have been masked by a greater reduction of PAG activity, given the limited resolution of the microPET technique.

In summary, the marked neurochemical (Gasull-Camós et al., 2017) and neuroimaging (present study) differences resulting from astroglial GLT-1 blockade in IL and PrL further enhance the relevance of astrocytes in modulating brain function and contribute to a better understanding of brain networks involved in fast antidepressant actions. The present data also warrant further investigation on the differential control of IL and PrL on serotonergic activity.

Acknowledgments

We thank Alexandra de Francisco and Yolanda Sierra for their support in animal handling and acquisition of imaging studies. We also thank María Jaramillo for administrative and managing assistance.

This work was supported by Spanish Ministry of Economy and Competitiveness grants (SAF2012-35183, SAF2015-68346, ISCIII-FIS PI14/00860 and CPII14/00005, and BES2013-063241 J.G.C.) cofinanced by European Regional Development Fund, Generalitat de Catalunya (2014-SGR798), Comunidad de Madrid (BRADE-CM S2013/ICE-2958), Mapfre foundation, Alicia Koplowitz Foundation (FAK16/01), and Centro de Investigación Biomédica en Red de Salud Mental.

Statement of Interest

F.A. has received consulting honoraria from Lundbeck A/S and has been PI of a grant from Lundbeck A/S. He is also a member of the scientific advisory board of Neurolixis and a co-inventor of 2 patents on conjugated oligonucleotide sequences. The remaining authors declare no conflict of interest.

References

Borghammer P, Aanerud J, Gjedde A (2009) Data-driven intensity normalization of PET group comparison studies is superior to global mean normalization. *NeuroImage* 46:981–988.

- Celada P, Puig MV, Casanovas JM, Guillazo G, Artigas F (2001) Control of dorsal raphe serotonergic neurons by the medial prefrontal cortex: involvement of serotonin-1A, GABA A, and glutamate receptors. *J Neurosci* 21:9917–9929.
- Chen J, Zhou C, Wu B, Wang Y, Li Q, Wei Y, Yang D, Mu J, Zhu D, Zou D, Xie P (2013) Left versus right repetitive transcranial magnetic stimulation in treating major depression: a meta-analysis of randomised controlled trials. *Psychiatry Res* 210:1260–1264.
- Dalley JW, Cardinal RN, Robbins TW (2004) Prefrontal executive and cognitive functions in rodents: neural and neurochemical substrates. *Neurosci Biobehav Rev* 28:771–784.
- Danbolt NC (2001) Glutamate uptake. *Prog Neurobiol* 65:1–105.
- Drevets WC, Price JL, Simpson Jr. JR, Todd RD, Reich T, Vannier M, Raichle ME (1997) Subgenual prefrontal cortex abnormalities in mood disorders. *Nature* 386:824–827.9.
- Fuchikami M, Thomas A, Liu R, Wohleb ES, Land BB, DiLeone RJ, Aghajanian GK, Duman RS (2015) Optogenetic stimulation of infralimbic PFC reproduces ketamine's rapid and sustained antidepressant actions. *Proc Natl Acad Sci U S A* 112:8106–8111.
- Gabbott PLA, Warner TA, Jays PRL, Bacon SJ (2003) Areal and synaptic interconnectivity of prelimbic (area 32), infralimbic (area 25) and insular cortices in the rat. *Brain Res* 993:59–71.
- Gabbott PLA, Warner TA, Jays PRL, Salway P, Busby SJ (2005) Prefrontal cortex in the rat: projections to subcortical autonomic, motor, and limbic centers. *J Comp Neurol* 492:145–177.
- Gasull-Camós J, Tarrés-Gatius M, Artigas F, Castañé A (2017) Glial GLT-1 blockade in infralimbic cortex as a new strategy to evoke rapid antidepressant-like effects in rats. *Transl Psychiatry* 7:e1038.
- Hadar R, Bikovski L, Soto-Montenegro ML, Schimke J, Maier P, Ewing S, Voget M, Wieske F, Götz T, Desco M, Hamani C, Pascau J, Weiner I, Winter C (2017) Early neuromodulation prevents the development of brain and behavioral abnormalities in a rodent model of schizophrenia. *Mol Psychiatry*:1–9.
- Hajós M, Richards CD, Székely AD, Sharp T (1998) An electrophysiological and neuroanatomical study of the medial prefrontal cortical projection to the midbrain raphe nuclei in the rat. *Neuroscience* 87:95–108.
- Harandi M, Agüera M, Gamrani H, Didier M, Maitre M, Calas A, Belin MF (1987) γ -Aminobutyric acid and 5-hydroxytryptamine interrelationship in the rat nucleus raphe dorsalis: combination of radioautographic and immunocytochemical techniques at light and electron microscopy levels. *Neuroscience* 21:237–251.
- Hoehn-Saric R, Schlaepfer TE, Greenberg BD, McLeod DR, Pearlson GD, Wong SH (2001) Cerebral blood flow in obsessive-compulsive patients with major depression: effect of treatment with sertraline or desipramine on treatment responders and non-responders. *Psychiatry Res* 108:89–100.
- Ji G, Neugebauer V (2012) Modulation of medial prefrontal cortical activity using *in vivo* recordings and optogenetics. *Mol Brain* 5:36.
- Li N, Lee B, Liu R-J, Banasr M, Dwyer JM, Iwata M, Li X-Y, Aghajanian G, Duman RS (2010) mTOR-dependent synapse formation underlies the rapid antidepressant effects of NMDA antagonists. *Science (New York, NY)* 329:959–964.
- Liu R, Jolas T, Aghajanian G (2000) Serotonin 5-HT₂ receptors activate local GABA inhibitory inputs to serotonergic neurons of the dorsal raphe nucleus. *Brain Res* 873:34–45.
- Mayberg HS, Lozano AM, Voon V, McNeely HE, Seminowicz D, Hamani C, Schwab JM, Kennedy SH (2005) Deep brain stimulation for treatment-resistant depression. *Neuron* 45:651–660.
- Oliveira JF, Sardinha VM, Guerra-Gomes S, Araque A, Sousa N (2015) Do stars govern our actions? Astrocyte involvement in rodent behavior. *Trends Neurosci* 38:535–549.

- Ongür D, Drevets WC, Price JL (1998) Glial reduction in the subgenual prefrontal cortex in mood disorders. *Proc Natl Acad Sci U S A* 95:13290–13295.
- Paxinos G, Watson C (2005) *The rat brain in stereotaxic coordinates*. Elsevier/Academic Press: Amsterdam, The Netherlands.
- Perea G, Araque A (2010) GLIA modulates synaptic transmission. *Brain Res Rev* 63:93–102.
- Romero A, Rojas S, Cabañero D, Gispert J, Herance J, Campillo A, Puig M (2011) A ¹⁸F-fluorodeoxyglucose MicroPET imaging study to assess changes in brain glucose metabolism in a rat model of surgery-induced latent pain sensitization. *Anesthesiology* 115:1072–1083.
- Seminowicz DA, Mayberg HS, McIntosh AR, Goldapple K, Kennedy S, Segal Z, Rafi-Tari S (2004) Limbic-frontal circuitry in major depression: a path modeling metanalysis. *Neuroimage* 22:409–418.
- Varga V, Székely AD, Csillag A, Sharp T, Hajós M (2001) Evidence for a role of GABA interneurons in the cortical modulation of midbrain 5-hydroxytryptamine neurones. *Neuroscience* 106:783–792.
- Vertes RP (2004) Differential projections of the infralimbic and prelimbic cortex in the rat. *Synapse (New York, NY)* 51:32–58.
- Wang QP, Ochiai H, Nakai Y (1992) GABAergic innervation of serotonergic neurons in the dorsal raphe nucleus of the rat studied by electron microscopy double immunostaining. *Brain Res Bull* 29:943–948.
- Warden MR, Selimbeyoglu A, Mirzabekov JJ, Lo M, Thompson KR, Kim S-Y, Adhikari A, Tye KM, Frank LM, Deisseroth K (2012) A prefrontal cortex-brainstem neuronal projection that controls response to behavioural challenge. *Nature* 492:428–432.
- Zanos P et al. (2016) NMDAR inhibition-independent antidepressant actions of ketamine metabolites. *Nature* 533:1–18.
- Zarate CA, Singh JB, Carlson PJ, Brutsche NE, Ameli R, Luckenbaugh DA, Charney DS, Manji HK (2006) A randomized trial of an NMDA antagonist in treatment-resistant major depression. *Arch Gen Psychiatry* 63:856–864.